Molecular Routes to Metal Oxides and Metal Silicates. Synthesis and Thermal Decomposition Studies of Eclipsed $Mo_2[O_2Si(O^tBu)_2]_3$ and $W_2(NHMe_2)_2[O_2Si(O^tBu)_2]_2[OSi(OH)(O^tBu)_2]_2$

Kai Su and T. Don Tilley*

Department of Chemistry, University of California, Berkeley, Berkeley, California 94720-1460, and the Chemical Sciences Division, Lawrence Berkeley Laboratory, 1 Cyclotron Road, Berkeley, California 94720

Received August 1, 1996. Revised Manuscript Received November 14, 1996[⊗]

Reaction of $Mo_2(NMe_2)_6$ with 3 equiv of $(^tBuO)_2Si(OH)_2$ afforded a new siloxide complex, $Mo_2[O_2Si(O^tBu)_2]_3$ (**1**), as the only metal-containing product. An X-ray crystal structure determination reveals that **1** adopts an eclipsed structure with three di-*tert*-butoxysilanediolato ligands bridging the molybdenum centers in a symmetrical fashion. Lewis acidic complex **1** forms an isolable adduct with pyridine. Reaction of $W_2(NMe_2)_6$ with 3 equiv of $(^tBuO)_2Si(OH)_2$ afforded $W_2(NHMe_2)_2[O_2Si(O^tBu)_2]_2[OSi(OH)(O^tBu)_2]_2$ (**3**), which was isolated as air-sensitive orange crystals. In this molecule, two $O_2Si(O^tBu)_2$ ligands bridge the W≡W bond in an η^1,η^1 fashion, and $OSi(OH)(O^tBu)_2$ ligands are coordinated to each W atom. This molecule adopts a highly eclipsed conformation and has a 2-fold axis of symmetry which perpendicularly bisects the tungsten−tungsten bond. Complex **1** undergoes a two-step weight loss (by TGA), which corresponds to the initial loss of isobutene and water (at ca. 200 °C), followed by the loss of molybdenum by evaporation of MoO_3 at 700−1050 °C. The pyrolysis of **1** at 550 °C for 2 h under argon gave a ceramic material with the approximate formula $Mo_2Si_3O_{10}$. When the sample was heated at 1200 °C for 1 h, evaporation of MoO_3 occurred and the final ceramic material had a composition of $Mo_{0.5}Si_3O_{6.5}$. Very low carbon contents for these materials are consistent with a clean elimination process during the pyrolysis. The material heated to 550 °C is amorphous, while the material taken to 1200 °C contains MoO_2 as the only crystalline phase. Pyrolysis of **1** in air at 1200 °C resulted in the extensive loss of molybdenum (2.14% Mo; no crystalline phases by XRD). Interestingly, pyrolysis of small crystals of **1** occurs with retention of the crystals' shape and size, despite a great loss in weight (75%). Pyrolysis of **3** at 550 and 1200 °C under argon produced ceramic materials consistent with the formulas $W_{2.2}Si_4O_{17.4}$ and $W_{2.2}Si_4O_{13}$, respectively. While the 550 °C ceramic is amorphous, the 1200 °C material contains crystalline W and WO_2 (by XRD analysis).

Introduction

The molecular precursor route to solid-state materials represents a novel synthetic strategy that is being explored in pursuit of new generations of advanced materials.[1,2] In recent years, we have been exploring a single-source precursor approach to various metal silicate materials based on tris(alkoxy)siloxy complexes of the type $M[OSi(O^tBu)_3]_n$. These oxygen-rich complexes undergo very clean conversions at remarkably low temperatures (100−200 °C) to amorphous, homogeneous, metal oxide−silica or metal silicate materials.[3] Typically, the ceramic conversions occur without the incorporation of carbon, which is often a problem associated with organometallic and polymer precursor routes to ceramics. We have also recently employed the di-*tert*-butoxysilanediolato ligand in the synthesis of a preceramic polymer, $[ZnOSi(O^tBu)_2O]_n$, which was used to obtain manganese-doped zinc orthosilicate phosphors.[4] Thus, this approach seems to represent a

* To whom correspondence should be addressed at the University of California, Berkeley.

⊗ Abstract published in *Advance ACS Abstracts,* January 1, 1997.

(1) For example see: (a) *Ultrastructure Processing of Advanced Materials;* Uhlmann, D. R., Ulrich, D. R., Eds.; Wiley-Interscience: New York, 1992. (b) *Better Ceramics Through Chemistry V;* Materials Research Society Symposia Proceedings; Hampden-Smith, M. J., Klemperer, W. G., Brinker, C. J., Eds.; Materials Research Society: Pittsburgh, 1992 Vol. 271. (c) *Inorganic Materials;* Bruce, D. W., O'Hare, D., Eds.; Wiley: New York, 1992. (d) Bowes, C. L.; Ozin, G. A. *Adv. Mater.* **1996**, *8,* 13. (e) Amabilino, D. B.; Stoddart, J. F. *Chem. Rev. (Washington, D.C.)* **1995**, *95,* 2725. (f) Stein, A.; Keller, S. W.; Mallouk, T. E. *Science* **1993**, *259,* 1558. (g) Hubert-Pfalzgraf, L. G. *New J. Chem.* **1987**, *11,* 663. (h) Mehrotra, R. C. *J. Non-Cryst. Solids* **1988**, *100,* 1. (i) Sanchez, C.; Livage, J.; Henry, M.; Babonneau, F. *J. Non-Cryst. Solids* **1988**, *100,* 165. (j) Chandler, C. D.; Roger, C.; Hampden-Smith, M. J. *Chem. Rev. (Washington, D.C.)* **1993**, *93,* 1205.

(2) References on the single-source precursor approach: (a) Cowley, A. H.; Jones, R. A. *Angew. Chem., Int. Ed. Engl.* **1989**, *28,* 1208. (b) Williams, A. G.; Interrante, L. V. In *Better Ceramics Through Chemistry;* Materials Research Society Symposia Proceedings; Brinker, C. J.; Clark, D. E.; Ulrich, D. R., Eds.; North-Holland: New York, 1984 Vol. 32, p 152. (c) Apblett, A. W.; Warren, A. C.; Barron, A. R. *Chem. Mater.* **1992**, *4,* 167. (d) Chaput, F.; Lecomte, A.; Dauger, A.; Boilot, J. P. *Chem. Mater.* **1989**, *1,* 199. (e) Hoffman, D. M. *Polyhedron* **1994**, *13,* 1169.

(3) (a) Terry, K. W.; Tilley, T. D. *Chem. Mater.* **1991**, *3,* 1001. (b) Terry, K. W. Ph.D. Thesis, University of California at San Diego, 1993. (c) Terry, K. W.; Gantzel, P. K.; Tilley, T. D. *Chem. Mater.* **1992**, *4,* 1290. (d) Terry, K. W.; Lugmair, C. G.; Gantzel, P. K.; Tilley, T. D. *Chem. Mater.* **1996**, *8,* 274. (e) Terry, K. W.; Lugmair, C. G.; Tilley, T. D., manuscript in preparation.

(4) Su, K.; Tilley, T. D.; Sailor, M. J. *J. Am. Chem. Soc.* **1996**, *118,* 3459.

S0897-4756(96)00413-9 CCC: $14.00

general method for the synthesis of tailored materials with various properties. In this paper, we describe possible molecular precursor routes to silica-supported molybdenum and tungsten materials, which are widely used as catalysts in a number of industrial processes.[5] In the first phase of this investigation, we have examined the synthesis of precursor complexes of molybdenum and tungsten containing the di-*tert*-butoxysilanediolato ligand. The pyrolytic conversion of these complexes to materials is also reported.

Experimental Section

All synthetic manipulations were performed under an atmosphere of nitrogen or argon using standard Schlenk techniques and/or a Vacuum Atmospheres drybox. Di-*tert*-butoxysilanediol[6] and $M_2(NMe_2)_3$ (M = Mo[7] and W[8]) were prepared according to literature procedures. Di-*tert*-butoxysilanediol was dried over Drierite in pentane for 0.5 h at room temperature and then crystallized from pentane before use. Pentane, toluene, and pyridine were freshly distilled from sodium benzophenone. The ceramic samples were handled in air.

Infrared spectra were obtained on a Mattson Galaxy Series Fourier transform spectrophotometer. ^{1}H (400.1 MHz) and ^{13}C (100.6 MHz) NMR spectra were obtained on a Bruker AMX 400 spectrometer equipped with the appropriate decoupling accessories. X-ray powder diffraction (XRD) spectra were recorded on a Sintag XDS 2000 X-ray diffractometer using Cu Kα radiation. The XRD peaks were indexed according to the JCPDS data files (1989), and all assignments are given in the text and/or figures. The observed XRD patterns compared well with the literature values. Scanning electron microscopy (SEM) was performed on a Cambridge S360 microscope. Transmission electron micrographs (TEM) were recorded on a JEOL 100 CX microscope. Thermal analyses were performed on a Dupont 951 2000 thermal analysis system. Elemental analyses were performed at Galbraith, Knoxville, TN 37921, or at the Robertson Microlit Laboratories, Madison, NJ 07940.

$Mo_2[O_2Si(O^tBu)_2]_3$ (1). A 100 mL Schlenk tube was charged with 0.96 g of $(^tBuO)_2Si(OH)_2$ (4.61 mmol), 0.70 g of $Mo_2(NMe_2)_6$ (1.54 mmol), and 20 mL of pentane. The reaction mixture was stirred for 0.5 h, and the solution was then concentrated to about 2 mL. Heating this solution at 50 °C for ca. 30 min resulted in deposition of light yellow, needlelike crystals that would not redissolve in pentane. The product was washed with 10 mL of pentane, and subsequent drying in vacuo gave 1.0 g (1.23 mmol, 80.4%) of analytically pure **1**. Anal. Calcd for $C_{24}H_{54}Mo_2O_{12}Si_3$: C, 35.55; H, 6.71. Found: C, 35.43; H, 6.72. ^{1}H NMR (benzene-d_6, containing $HNMe_2$ from the reaction mixture, 400.1 MHz) δ 1.54 (s, 54 H, $OCMe_3$). ^{13}C{^{1}H} NMR (benzene-d_6, containing $HNMe_2$ from the reaction mixture, 100.6 MHz) δ 31.2 ($OCMe_3$), 73.4 ($OCMe_3$). IR (Nujol, NaCl, cm^{-1}) 2996 vs, 2930 s, 2848 s, 1463 s, 1389 s, 1258 m, 1217 m, 1200 m, 1085 m, 880 m, 839 m, 807 m, 733 w, 676 w, 659 w, 585 m, 520 w.

$Mo_2[O_2Si(O^tBu)_2]_3(pyr)_2$ (2). A Schlenk flask was charged with $(^tBuO)_2Si(OH)_2$ (0.30 g, 1.44 mmol), $Mo_2(NMe_2)_6$ (0.22 g, 0.48 mmol), and pentane (10 mL). To the resulting solution was added 0.5 mL of pyridine. After the solution was stirred at room temperature for 0.5 h, it was concentrated to about 1 mL and cooled to −78 °C to afford 0.24 g (0.25 mmol, 52.1%) of the product as yellow-brown crystals. Anal. Calcd for $C_{34}H_{64}Mo_2N_2O_{12}Si_3$: C, 42.14; H, 6.61; N, 2.89. Found: C, 40.93, H, 6.91, N, 3.54. ^{1}H NMR (benzene-d_6, 400.1 MHz) δ 8.57 (d, J = 4.3 Hz, 4 H, pyr), 7.69 (t, J = 7.6 Hz, 2 H, pyr), 7.28 (m, 4 H, pyr), 1.43 (s, 54 H, $OCMe_3$). ^{13}C{^{1}H} NMR (benzene-d_6, 100.6 MHz) δ 31.4 ($OCMe_3$), 73.3 ($OCMe_3$), 123.6, 136.1, 149.5 (pyr). IR (Nujol, NaCl, cm^{-1}) 2943 vs, 2912 s, 2858 vs, 1612 w, 1465 m, 1372 m, 1249 m, 1202 m, 1047 s, 1032 s, 947 w, 839 s, 838 w, 815 w, 769 w, 715 m, 653 w, 585 w, 552 m, 506 m, 428 w.

$W_2(NHMe_2)_2[O_2Si(O^tBu)_2]_2[OSi(OH)(O^tBu)_2]_2$ (3). A pentane (8 mL) solution of $(^tBuO)_2Si(OH)_2$ (0.99 g, 4.76 mmol) was added quickly to a 20 mL pentane solution of $W_2(NMe_2)_6$ (1.0 g, 1.58 mmol) at room temperature. After the reaction mixture was stirred for 10 min, the solvent was evaporated under vacuum to produce an orange-yellow, crystalline solid. A 1.05 g sample (0.98 mmol, 62.0%) of the product was obtained after washing with cold pentane at −30 °C. Anal. Calcd for $C_{36}H_{88}N_2O_{16}Si_4W_2$: C, 33.65; H, 6.90; N, 2.18. Found: C, 32.70; H, 7.27; N, 2.15. ^{1}H NMR (benzene-d_6, 400.1 MHz) δ 1.37 (s, 18 H, $OCMe_3$), 1.63 (s, 18 H, $OCMe_3$), 2.49 (d, J_{HH} = 6.4 Hz, 6 H, $NHMe_2$), 3.70 (br, 2 H, $NHMe_2$), 5.05 (s, 2 H, OH). ^{13}C{^{1}H} NMR (benzene-d_6, 100.6 MHz) δ 31.6 ($OCMe_3$), 32.0 ($OCMe_3$), 41.5 ($NHMe_2$) 72.2 ($OCMe_3$), 73.0 ($OCMe_3$). IR (Nujol, NaCl, cm^{-1}) 3431 m, 3229 w, 2993 s, 2866 s, 1480 m, 1459 m, 1400 m, 1374 s, 1256 s, 1206 s, 1071 vs, 1029 s, 974 s, 911 s, 877 s, 869 s, 835 w, 810 m, 708 m, 666 w, 641 w, 548 s, 523 s, 481 w, 439 w.

Solid-State Thermolysis of 1. In a typical procedure, a sample of **1** was weighed into a zirconia crucible in an inert atmosphere glovebox and then quickly transferred to a Lindberg tube furnace under a counter flow of argon. The furnace was then purged with argon for an additional 10 min before heating was initiated. Under a continuous flow of argon, 0.15 and 0.34 g samples were heated to 550 and 1200 °C, respectively, at 10 °C/min. Each temperature was maintained for 1 h before the samples were allowed to cool to room temperature. These pyrolyses yielded 0.08 (53%) and 0.09 g (26%) of ceramic samples, respectively. Anal. Found for sample heated to 550 °C: C, 0.66; H, 0.50; Mo, 42.22; Si, 18.90. For sample heated to 1200 °C: C, 0.04; H, 0.03; Mo, 20.99; Si, 35.27. The infrared spectrum of this material contained only a broad, featureless absorption band centered at 1000 cm^{-1}.

Pyrolyses of 0.17 and 0.15 g of **1** in dry air for 1 h at 550 and 1200 °C (10 °C/min) yielded 0.10 (58.8%) and 0.035 g (23.3%) of ceramic samples, respectively. Anal. Found for sample heated to 550 °C: C, 0.05%; H, 0.41%. For sample heated to 1200 °C: Mo, 2.14%; Si, 43.71%. Surface area for sample heated to 550 °C in air: 43 m^2 g^{-1}.

Solid-State Thermolysis of 3. The method used above for **1** was employed. Under a continuous flow of argon, 0.37 and 0.35 g samples were heated to 550 and 1200 °C, respectively, at 10 °C/min. Each temperature was maintained for 1 h before the samples were allowed to cool to room temperature. These pyrolyses yielded 0.21 (56.8%) and 0.174 g (49.7%) of ceramic samples, respectively. Anal. Found for sample heated to 550 °C: C, 1.72%; H, 0.22%; W, 50.15%; Si, 13.75%. For sample heated to 1200 °C: C, 0.48%; H, <0.01%; W, 54.92%; Si, 15.64%.

NMR Studies of Ceramic Conversion Reactions. Samples of **1** (68.4 mg) and **3** (58.0 mg) were placed in Schlenk tubes, and each tube was heated to 350 °C for 30 min under static vacuum. The volatile decomposition products were vacuum-transferred at −196 °C into an NMR tube containing benzene-d_6 and ferrocene standard. The volatile products were quantified via integrations against the internal standard. **1**: CH_2=CMe_2, 32.3 mg; ^{t}BuOH, trace; residual ceramic, 25 mg. **3**: CH_2=CMe_2, 15.8 mg; ^{t}BuOH, 3.54 mg; Me_2NH, 4.51 mg; residual ceramic, 27 mg.

Structure Determinations for 1 and 3. Clear, light yellow needle crystals of **1** were obtained by slow crystallization at 35−40 °C from a reaction mixture. A crystal was mounted on a glass fiber using Paratone N hydrocarbon oil. X-ray intensity data were collected at −108 °C on an Enraf-

(5) (a) *Transition Metal Oxides: Surface Chemistry and Catalysis*; Kung, H. H.; Elsevier: Amsterdam, 1989. (b) Kim, D. S.; Ostromecki, M.; Wachs, I. E.; Kohler, S. D.; Ekerdt, J. G. *Catal. Lett.* **1995**, *33*, 209. (c) Sullivan, D. L.; Roark, R. D.; Ekerdt, J. G.; Deutsch, S. E.; Gates, B. C. *J. Phys. Chem.* **1995**, *99*, 3678. (d) Suzuki, K.; Hayakawa, T.; Shimizu, M.; Takehira, K. *Catal. Lett.* **1995**, *30*, 159. (e) Banares, M. A.; Hu, H. C.; Wachs, I. E. *J. Catal.* **1995**, *155*, 249. (f) Williams, C. C.; Ekerdt, J. G. *J. Catal.* **1993**, *141*, 430. (g) Elev, I. V.; Shelimov, B. N.; Kazanskii, V. B. **1989**, *30*, 787 and references therein.

(6) Miner, C. S., Jr.; Bryan, L. A.; Holysz, R. P.; Pedlow, G. W., Jr. *Ind. Eng. Chem.* **1947**, *39*, 1368.

(7) Chisholm, M. H.; Cotton, F. A.; Frenz, B. A.; Reichert, W. W.; Shive, L. W.; Stults, B. R. *J. Am. Chem. Soc.* **1976**, *98*, 4469.

(8) Chisholm, M. H.; Cotton, F. A.; Extine, M. W.; Stults, B. R. *J. Am. Chem. Soc.* **1976**, *98*, 4477.

Table 1. Crystallographic Data for Compounds 1 and 3

	1	3
	(a) Crystal Parameters	
formula	$C_{24}H_{54}Mo_2O_{12}Si_3$	$C_{36}H_{86}N_2O_{16}Si_4W_2$
formula weight	810.8	1283.12
space group	*Cc*	$P2_1/n$
a (Å)	25.051(4)	11.8142(2)
b (Å)	14.358(3)	15.8712(2)
c (Å)	10.998(2)	14.7137(1)
β (deg)	112.88(1)	95.585(1)
V (Å^3)	3644(2)	2745.80(5)
Z	4	2
cryst color	colorless	yellow
D(calc), g cm^{-3}	1.48	1.552
μ (MoK_α), cm^{-1}	8.2	43.4
temp, °C	−108	−123
	(b) Data Collection	
diffractometer	Enraf-Nonius CAD−4	Siemens SMART
monochromator	graphite	graphite
radiation	Mo Kα (λ = 0.710 73 Å)	Mo Kα (λ = 0.710 69 Å)
scan type	$2\theta-\theta$	ω (0.3°/frame)
rflns collected	2987	10688
indpt rflns	2857	4060
	(c) Refinement	
R(F), %	3.62	4.4
R(wF), %	4.19	5.0
$\Delta(\rho)$, e Å^{-3}	0.82	2.41
GOF	1.755	1.92

Nonius CAD-4 diffractometer equipped with a nitrogen flow low-temperature apparatus which was previously calibrated by a thermocouple placed at the sample position. Crystallographic data are listed in Table 1. Automatic peak search and indexing procedures yielded a triclinic reduced primitive cell. Inspection of the Niggli values revealed a monoclinic C-centered cell. The unique raw intensity data were converted to structure factor amplitudes and their esd's by correction for scan speed, background, Lorentz, and polarization effects. No correction for crystal decomposition was necessary. Inspection of the azimuthal scan data for **1** showed a variation which suggested that the crystal was moving during the data collection. An empirical correction was made to the data based on the combined difference of F_{obs} and F_{calc}, following refinement of all atoms with isotropic thermal parameters (T_{max} = 1.10, T_{min} = 0.79, no θ dependence). The structure of **1** was solved by Patterson methods in space group *C*2/*c* and refined via standard least-squares and Fourier techniques. Initial refinement in the centric space group with a 2-fold axis through the molecule indicated profound disorder in the ligands, or a lower symmetry. Transferring the refinement to space group *Cc* produced the well-ordered and well-behaved model reported here. Hydrogen atoms attached to ordered carbon atoms were assigned idealized locations and values of B_{iso} approximately 1.25 times the B_{eqv} of the atoms to which they were attached. They were included in structure factor calculations but not refined.

Orange-yellow crystals of **3** were obtained by slow evaporation of a benzene solution at room temperature. A crystal was mounted on a glass fiber using Paratone N hydrocarbon oil. Data were collected using a Siemens SMART diffractometer with a CCD area detector. A hemisphere of data was collected at −123 °C using ω scans of 0.3° and a collection time of 30 s/frame. Systematic absences uniquely defined the space group as $P2_1/n$ (No. 14). The frame data were integrated using the program SAINT (SAX Area-Detector Integration Program; V4.024; Siemens Industrial Automation, Inc.: Madison, WI, 1995), with box parameters of 2.4 × 2.4 × 0.9°. The data were corrected for Lorentz and polarization effects. No decay correction was necessary. An empirical absorption correction based on measurements of multiply redundant data was performed using the program XPREP (part of the SHELXTL Crystal Structure Determination Package; Siemens Industrial Automation, Inc.: Madison, WI, 1995; μR = 0.2, T_{max} = 0.64, T_{min} = 0.34). The 10 688 integrated reflections were averaged in the point group 2/*m* to yield 4060 unique reflections (R_{int} = 0.071). The structure was solved by direct methods and expanded using Fourier techniques. All non-hydrogen atoms were refined anisotropically. Hydrogen atoms were included in calculated positions but not refined. The final cycle of full-matrix least-squares refinement was based on 2884 observed reflections ($I > 3.00\sigma(I)$). The maximum and minimum peaks on the final difference Fourier map corresponded to 1.50 and −2.41 e$^-$/Å^3, respectively. All calculations were performed using the teXsan crystallographic software package of the Molecular Structure Corp.

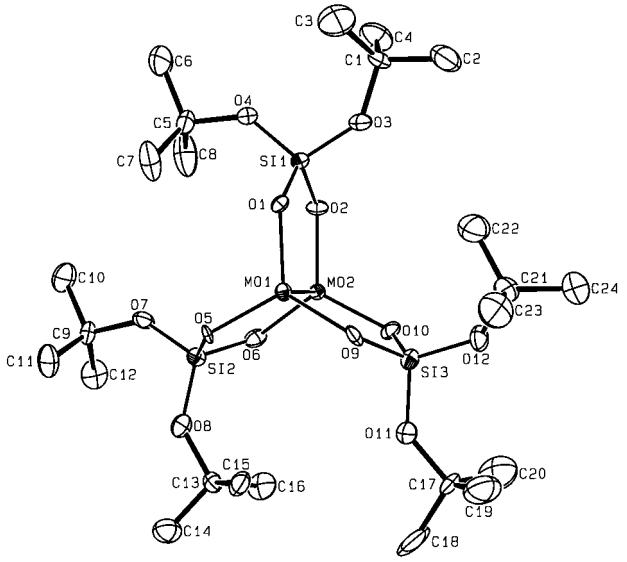

Figure 1. ORTEP drawing of $Mo_2[O_2Si(O^tBu)_2]_3$ (**1**).

Results and Discussion

Synthesis of Molybdenum and Tungsten Siloxide Complexes. Reaction of 3 equiv of $(^tBuO)_2Si(OH)_2$ with $Mo_2(NMe_2)_6$ in pentane solution at room temperature afforded a new Mo siloxide complex $Mo_2[O_2Si(O^tBu)_2]_3$ (**1**, eq 1). This species is insoluble in hydrocarbon

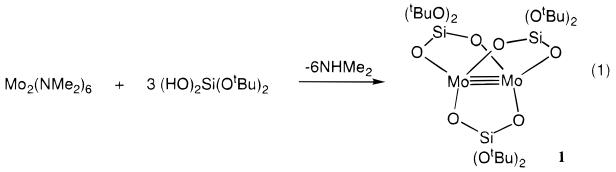

solvents but is solubilized by donors such as dimethylamine. Thus, **1** is soluble in the reaction solution, from which it slowly crystallizes as the base-free complex at room temperature. The reaction may be monitored by ^{1}H NMR spectroscopy, which indicates that the product forms quantitatively in benzene-d_6 solution. Compound **1** was isolated as light yellow, moderately air-stable, needlelike crystals from a concentrated reaction solution at 40−50 °C.

The molecular structure of **1** is shown in the ORTEP drawing of Figure 1, and selected bond distances and angles are given in Table 2. Molecules in the unit cell are related by a crystallographic *c*-glide, and interact via intermolecular Mo···O interactions which create chains running along the *c*-axis. The intermolecular contacts result in Mo(1)···O(2) and Mo(2)···O(5) distances of 2.75 and 2.69 Å, respectively. These contacts are too long to be considered normal bonds but clearly represent significant interactions. A similar structure involving intermolecular metal···ligand interactions has

Table 2. Selected Bond Distances (Å) and Angles (Deg) for $Mo_2[O_2Si(O^tBu)_2]_3$ (1)

(a) Bond Distances

Mo1−Mo2	2.240(1)	Si1−O3	1.620(8)
Mo1−O1	1.906(7)	Si1−O4	1.606(7)
Mo1−O5	1.933(8)	Si2−O5	1.665(9)
Mo1−O9	1.910(7)	Si2−O6	1.630(9)
Mo2−O2	1.930(8)	Si2−O7	1.612(8)
Mo2−O6	1.903(8)	Si2−O8	1.586(8)
Mo2−O10	1.883(8)	Si3−O9	1.646(9)
Mo1···O2′[a]	2.752(9)	Si3−O10	1.650(9)
Mo2···O5′[a]	2.691(8)	Si3−O11	1.596(9)
Si1−O1	1.644(8)	Si3−O12	1.611(8)
Si1−O2	1.648(9)		

(b) Bond Angles

Mo2−Mo1−O1	96.1(2)	O2−Si1−O4	112.2(4)
Mo2−Mo1−O5	96.1(3)	O3−Si1−O4	110.0(4)
Mo2−Mo1−O9	95.3(3)	O5−Si2−O6	105.3(4)
Mo1−Mo2−O2	95.2(3)	O5−Si2−O7	109.6(4)
Mo1−Mo2−O6	95.1(3)	O5−Si2−O8	111.5(4)
Mo1−Mo2−O10	96.1(3)	O6−Si2−O7	106.5(4)
O1−Mo1−O5	117.4(3)	O6−Si2−O8	114.2(4)
O1−Mo1−O9	118.4(3)	O7−Si2−O8	109.5(4)
O5−Mo1−O9	121.1(3)	O9−Si3−O10	105.2(3)
O2−Mo2−O6	121.8(3)	O9−Si3−O11	108.4(5)
O2−Mo2−O10	118.4(3)	O9−Si3−O12	112.7(5)
O6−Mo2−O10	117.1(3)	O10−Si3−O11	108.7(5)
Mo1−O1−Si1	121.8(4)	O10−Si3−O12	112.0(4)
Mo2−O2−Si1	121.4(5)	O11−Si3−O12	109.8(4)
Mo1−O5−Si2	120.0(5)	Si1−O3−C1	138.1(7)
Mo2−O6−Si2	122.9(5)	Si1−O4−C5	135.5(7)
Mo1−O9−Si3	121.3(5)	Si2−O7−C9	136.1(7)
Mo2−O10−Si3	121.6(4)	Si2−O8−C13	136.1(6)
O1−Si1−O2	105.3(4)	Si3−O11−C17	136.5(8)
O1−Si1−O3	107.9(5)	Si3−O12−C21	135.2(8)
O1−Si1−O4	112.0(4)	Mo2−Mo1···O2′[a]	167.3(2)
O2−Si1−O3	109.3(5)	Mo1−Mo2···O5′[a]	167.6(2)

[a] O2′ and O5′ are in the neighboring molecules, and related to the original molecule by the crystallographic *c*-glide.

been observed for $W_2(OCMe_2CMe_2)_3$.[9] An unusual feature of **1** is its eclipsed geometry; the approximate 3/*m* symmetry is broken primarily by displacement of some of the ^{t}Bu groups out of the noncrystallographic mirror plane. The Mo1−Mo2−O2−Si1−O1, Mo1−Mo2−O10−Si3−O9, and Mo1−Mo2−O6−Si2−O5 five-membered rings are quite planar, and the dihedral angles between these planes are very close to 120° (119.4−120.3°). The coordination geometries for the molybdenum centers may be described as tetrahedrons which are severely distorted toward trigonal-based pyramids, with the Mo atoms lying barely (0.195, 0.180 Å) out of their O_3 coordination planes. The Mo−Mo distance, 2.240(1) Å, is similar to the comparable distance found in related dimolybdenum compounds.[10] The remaining bond distances and angles are normal and similar to those observed in related trialkoxysiloxy complexes.[3c,d,e,4]

The structure of **1** is interesting in light of long-standing discussions concerning the most stable conformations for $X_3M{\equiv}MX_3$ compounds.[11−14] In 1978, Albright and Hoffmann suggested that triply bonded d^3-d^3 dimers of this type should have an electronic preference for an eclipsed geometry. The preponderance of staggered geometries observed for such dimers was attributed to a purely steric factor.[11] Chisholm and coworkers have reported a number of nearly eclipsed compounds possessing ligands that bridge a Mo_2^{6+} or W_2^{6+} core to form six-membered chelate rings.[12−15] For example, $Mo_2(MeNCH_2CH_2NMe)_3$ exhibits N−Mo−Mo−N torsion angles which average to 12°.[13] Generally, it has been found that the M_2X_6 conformation has little influence on distances and angles in the complexes, or on their electronic properties. The highly eclipsed geometry for **1** (average O−Mo−Mo−O torsion angle = 3°) may be due at least partly to the presence of planar, five-membered chelate rings, whose distortion may result in considerable ring strain.

Reaction of 3 equiv of $(^tBuO)_2Si(OH)_2$ with $Mo_2(NMe_2)_6$ in the presence of pyridine afforded a pyridine adduct of **1**, which was isolated in moderate yield as deep orange crystals (eq 2). In contrast to **1**, the

$$Mo_2(NMe_2)_6 + 3(HO)_2Si(O^tBu)_2 \xrightarrow[-6NHMe_2]{2pyr} \underset{\mathbf{2}}{Mo_2[O_2Si(O^tBu)_2]_3(pyr)_2} \quad (2)$$

pyridine adduct **2** is readily soluble in hydrocarbons such as benzene. The molecular formula for **2** was established by combustion analysis and NMR spectroscopy. Note that similar adducts were not isolated after **1** was crystallized in the presence of either $HNMe_2$ or PMe_3. However, the increased solubility of **1** in hydrocarbon solvents in the presence of the latter donors suggests an association/dissociation equilibrium in solution. The exact structure of **2** has not been determined. A related complex, $W_2(O^iPr)_6(pyr)_2$, has been characterized as having a structure consisting of nearly planar $W(O^iPr)_3(pyr)$ units in a staggered conformation.[16] However, complex **2** may adopt a somewhat different structure given the steric constraints imposed by the silanediolato chelate rings.

The reaction of $W_2(NMe_2)_6$ with 3 or 4 equiv of $(^tBuO)_2Si(OH)_2$ afforded a new complex, $W_2(NHMe_2)_2[O_2Si(O^tBu)_2]_2[OSi(OH)(O^tBu)_2]_2$ (**3**; >85% by ^{1}H NMR

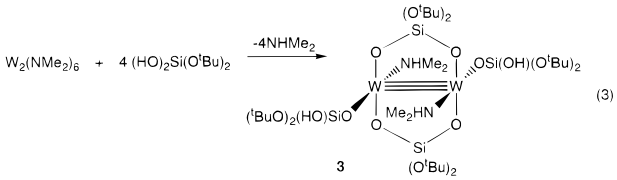

(3)

spectroscopy), along with minor unidentified side products. Compound **3** was isolated as air-sensitive deep orange crystals that are only moderately soluble in pentane but readily soluble in benzene. The complex slowly decomposes in solution at room temperature, therefore isolation must be performed immediately following completion of the reaction.

The structure of **3** was determined by a single-crystal X-ray diffraction study, and is illustrated by the ORTEP diagram of Figure 2. Selected bond distances and angles are listed in Table 3. There are two crystallo-

(9) Chisholm, M. H.; Folting, K.; Hampden-Smith, M.; Smith, C. A. *Polyhedron* **1987**, *6*, 1747.
(10) Chisholm, M. H.; Cotton, F. A. *Acc. Chem. Soc.* **1977**, *11*, 356.
(11) Albright, T. A.; Hoffmann, R. *J. Am. Chem. Soc.* **1978**, *100*, 7736.
(12) Blatchford, T. P.; Chisholm, M. H.; Folting, K.; Huffman, J. C. *Inorg. Chem.* **1980**, *19*, 3175.
(13) Blatchford, T. P.; Chisholm, M. H.; Huffman, J. C. *Inorg. Chem.* **1987**, *26*, 1920.
(14) Chisholm, M. H.; Folting, K.; Hampden-Smith, M.; Smith, C. A. *Polyhedron* **1987**, *6*, 1747.
(15) Chisholm, M. H.; Folting, K.; Haubrich, S. T.; Martin, J. D. *Inorg. Chim. Acta* **1993**, *213*, 17.
(16) Akiyama, M.; Chisholm, M. L.; Cotton, F. A.; Extine, M. W.; Haitko, D. A.; Little, D.; Fanwick, P. E. *Inorg. Chem.* **1979**, *18*, 2266.

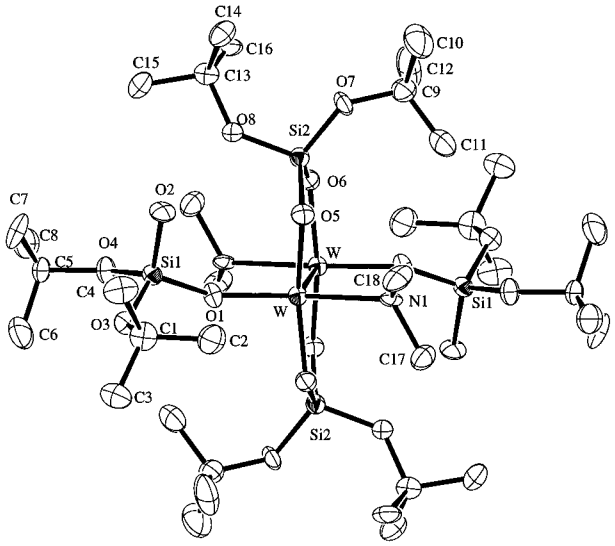

Figure 2. ORTEP drawing of $W_2(NHMe_2)_2[O_2Si(O^tBu)_2]_2[OSi(OH)(O^tBu)_2]_2$ (**3**).

graphically independent (but very similar) molecules in the unit cell. Two silanediolato ligands bridge the ditungsten center in an η^1,η^1 fashion, and the two di-*tert*-butoxy(hydroxy)siloxy ligands are linked to each tungsten atom via terminal W−O bonds. The molecules possess a center of symmetry, and the presence of $NHMe_2$ (vs $-NMe_2$) groups is supported by a pyramidal geometry at nitrogen. This interpretation is also consistent with the rather long W−N(1) bond of 2.260(8) Å, which is identical with the W−N bond distances observed in $W_2(O^iPr)_6(pyr)_2$.[16] Unlike most other structurally characterized $W_2X_6L_2$ complexes which possess a staggered geometry,[15] **3** adopts a highly eclipsed conformation. The W−W−O(5)−Si(2)−O(6) five-membered ring is quite planar, and forms angles of 89.2° and 88.9° with the W−O(1)−N(1)−W and O(1)−O(5)−O(6)−N(1) least-squares planes, respectively. Another molecule which possesses the unusual eclipsed geometry is $W_2(O^tBu)_4(OSO_2CF_3)_2(PMe_3)_2$, which has torsion angles about the W−W bond ranging from 6.7 to 10.1°.[17] The latter compound has a long W≡W bond distance of 2.421(1) Å, while **3** has a more typical bond length of 2.2805(8) Å.[10]

The infrared spectrum of **3** supports the presence of unreacted OH and/or NH groups, as strong absorptions near 3000 cm^{-1} are clearly evident. The proton NMR spectrum of **3** exhibits resonances arising from two sets of equivalent $-O^tBu$ groups at 1.37 and 1.63 ppm, and a singlet at 5.05 ppm for the OH proton. A doublet at 2.49 ppm (J_{HH}, 6.4 Hz) and a broad peak at 3.70 ppm are assigned to the two Me_2NH ligands in each molecule. Also, the ^{13}C NMR spectrum shows peaks that can be attributed to two sets of $-O^tBu$ groups and one type of $HNMe_2$ ligand.

The different type of product observed for **3** (vs **1**) is consistent with the previously established greater tendency for tungsten to adopt higher coordination numbers by addition of neutral donor ligands to the W≡W core.[16] Previously reported products from reactions of $W_2(NMe_2)_6$ with silanols include $W_2(OSiPh_3)_4(NMe_2)_2$[18] and thermally unstable $W_2(OSiMe_3)_6(NHMe_2)_2$.[16] The reaction to give **3** may be contrasted with the reaction of $W_2(O^tBu)_6$ with pinacol, which produces $W_2(OCMe_2CMe_2O)_3$.[9]

Table 3. Selected Bond Distances (Å) and Angles (Deg) for $W_2(NHMe_2)_2[O_2Si(O^tBu)_2]_2[OSi(OH)(O^tBu)_2]_2$ (3)

(a) Bond Distances			
W−W	2.2805(8)	Si1−O3	1.628(7)
W−O1	1.932(6)	Si1−O4	1.614(7)
W−O5	1.972(7)	Si2−O5	1.622(7)
W−O6	1.975(7)	Si2−O6	1.635(7)
W−N1	2.260(8)	Si2−O7	1.623(7)
Si1−O1	1.604(7)	Si2−O8	1.642(7)
Si1−O2	1.638(7)		
(b) Bond Angles			
W−W−O1	101.7(2)	O2−Si1−O4	113.8(4)
W−W−O5	94.1(2)	O3−Si1−O4	107.1(4)
W−W−O6	95.6(2)	O5−Si2−O6	108.4(4)
W−W−N1	98.2(2)	O5−Si2−O7	114.3(4)
O1−W−O5	92.9(3)	O5−Si2−O8	103.0(4)
O1−W−O6	95.8(3)	O6−Si2−O7	113.0(4)
O1−W−N1	159.6(3)	O6−Si2−O8	111.9(4)
O5−W−O6	165.3(3)	O7−Si2−O8	105.9(4)
O5−W−N1	81.4(3)	W−O1−Si1	149.3(4)
O6−W−N1	86.4(3)	W−O5−Si2	120.2(4)
O1−Si1−O2	109.4(4)	W−O6−Si2	119.2(4)
O1−Si1−O3	114.4(4)	W−N1−C17	117.6(6)
O1−Si1−O4	104.2(4)	W−N1−C18	113.8(6)
O2−Si1−O3	108.1(4)		

Solid-State Thermolysis of $Mo_2[O_2Si(O^tBu)_2]_3$ (1). The pyrolytic conversion of **1** to ceramic materials was examined under various conditions. We anticipated that **1** would serve as a useful precursor to molybdosilicate materials, since related $-OSi(O^tBu)_3$ complexes have been observed to undergo clean elimination of organic groups under mild conditions to homogeneous metal silicate materials.[3,4,19]

Complex **1** exhibits a rather high thermal stability relative to most other metal *tert*-butoxysiloxy complexes. A thermal gravimetric analysis (TGA) trace for **1** under argon (Figure 3a) shows an initial, precipitous weight loss occurring at ca. 200 °C. The overall ceramic conversion process occurs in a stepwise fashion, with the first step completed by ca. 220 °C and resulting in a 55.4% ceramic yield. The second weight loss, occurring between 700 and 1050 °C, is more gradual and appears to correspond to the evaporation of MoO_3 (vide infra).[20] Loss of MoO_3 is signaled by an endothermic event at about 800 °C, as detected by differential thermal analysis (DTA). The TGA trace for **1** in dry air is similar to the one obtained under argon (Figure 3b), except that the second weight loss is greater. We presume that this results from the oxidation of molybdenum species to volatile MoO_3 under these conditions. The ceramic yields for the two weight losses under air are 59 and 25%.

The stoichiometry for the thermal decomposition of **1** at 300 °C was established by trapping the volatile decomposition products under vacuum. The volatile products, condensed into an NMR tube containing benzene-d_6 and a measured amount of ferrocene standard at −196 °C, were shown by ^1H NMR spectroscopy

(17) Chisholm, M. H.; Kramer, K. S.; Martin, J. D.; Huffman, J. C.; Lobkovsky, E. B.; Streib, W. E. *Inorg. Chem.* **1992**, *31*, 4469.

(18) Chisholm, M. H.; Parkin, I. P.; Huffman, J. C.; Lobkovsky, E. M.; Folting, K. *Polyhedron* **1991**, *10*, 2839.

(19) (a) Abe, Y.; Gunji, T.; Kimata, Y.; Kuramata, M.; Kasgöz, A.; Misono, T. *J. Non-Cryst. Solids* **1990**, *121*, 21. (b) Gunji, T.; Nagao, Y.; Misono, T.; Abe, Y. *J. Polym. Sci.: Part A: Polym. Chem.* **1991**, *29*, 941. (c) Gunji, T.; Nagao, Y.; Misono, T.; Abe, Y. *J. Polym. Sci.: Part A: Polym. Chem.* **1992**, *30*, 371.

(20) *Molybdenum. An Outline of Its Chemistry and Uses;* Braithwaite, E. R., Haber, J., Eds.; Elsevier: Amsterdam, 1994; p 14.

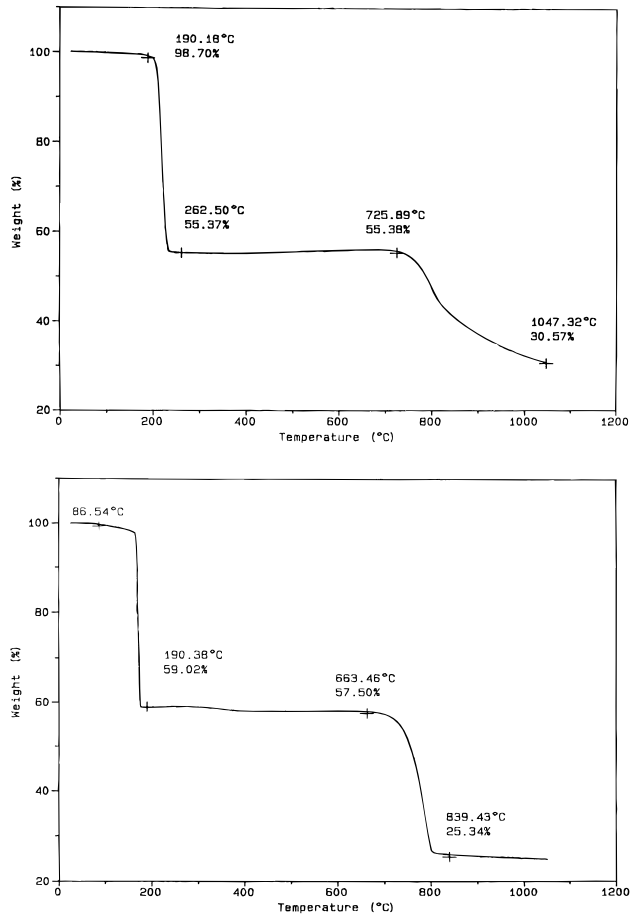

Figure 3. Thermal gravimetric analysis (TGA) trace for $Mo_2(O_2Si(O^tBu)_2)_3$ (**1**) (a, top) in argon and (b, bottom) in air.

to be approximately 6 equiv of isobutene and a slight trace of ^{t}BuOH. Therefore the solid-state thermolysis may be approximately described by eq 4. The nature

$$\underset{\mathbf{1}}{Mo_2[O_2Si(O^tBu)_2]_3} \xrightarrow{\Delta} \text{“}Mo_2Si_3O_9\text{”} + 3H_2O + 6CH_2{=}CMe_2 \quad (4)$$

of the molybdenum-containing fraction formed at this temperature, which should have an average composition of “$Mo_2Si_3O_9$”, is unknown. The theoretical yield associated with this process is 51.8%, which is slightly lower than the observed ceramic yield of 55.4% at 300 °C. The somewhat higher ceramic yield observed at 300 °C in air (ca. 59%) suggests some incorporation of oxygen, with formation of MoO_2 and/or MoO_3.

Bulk pyrolyses of **1** at 550 and 1200 °C under argon afforded black/gray ceramics in 53.3% and 26.5% ceramic yields, respectively. The composition of the material obtained by pyrolysis at 550 °C is approximately $Mo_2Si_3O_{10}$, based on an elemental analysis. A slight excess of oxygen could be due to oxidation of the material by trace amounts of oxygen in the argon. This material has very low carbon and hydrogen contents of 0.66% and 0.50%, respectively. A significant decrease in the molybdenum content was observed when the pyrolysis was carried out at 1200 °C. This material exhibited a composition of $Mo_{0.5}Si_3O_{6.5}$, as determined by elemental analysis, and a further reduction of the carbon and hydrogen contents was observed. The significant loss of molybdenum at high temperature is attributed to the evaporation of MoO_3, which is known to occur above ca. 800 °C.[20]

Pyrolysis of **1** in dry air at 550 and 1200 °C afforded white ceramics in 58.8 and 23.3% ceramic yields, respectively. The carbon and hydrogen levels for the material taken to 1200 °C, 0.04 and 0.03%, respectively, are quite low, and the material formed at this temperature has the formula $Mo_{0.04}Si_3O_{6.5}$ (2.14% Mo by weight). The more extensive loss of molybdenum during the pyrolysis in air provides further evidence for oxidation of molybdenum species to MoO_3, which is lost by evaporation. The observed ceramic yield (23.3%) is also consistent with formation of a ceramic material which is principally composed of SiO_2 (theoretical ceramic yield: 22.2%).

The transformations described above were also monitored by X-ray powder diffraction (XRD) analyses. Representative powder patterns are shown in Figure 4. Material taken to 550 °C under argon is amorphous (Figure 4a), but heating to 1200 °C under argon results in crystallization of MoO_2 (Figure 4b). In air, more of the molybdenum is oxidized and lost as vaporized MoO_3. Therefore at this temperature, no crystalline phases are detected by XRD (Figure 4c).

The low carbon contents observed for the materials obtained from **1** are consistent with what we have observed earlier for alkoxysiloxy complexes.[3,4] Such compounds have been observed to function as efficient ceramic precursors to carbon-free materials, presumably because of the “preformed” oxygen environments for both the metal and silicon atoms. No metal carbide species were detected by XRD. It is interesting to compare results that have been reported for the related dimolybdenum and ditungsten alkoxide complexes $M_2(OCy)_6$ and $W_2(CH_2Ph)_2(O^iPr)_4$, which give metal carbides upon thermolysis.[21] These compounds undergo two-step weight losses with TGA traces that are quite similar to those shown for compound **1** (Figure 3). However, this behavior was attributed to initial decomposition to an intermediate “$M_2C_4O_4$” phase, which decomposes further at higher temperature to M_2C metal carbides. $Mo_2(O^tBu)_6$ gives principally MoO_2 upon thermolysis, and $W_2(O^iPr)_6$ thermally decomposes to a mixture of W and WO_2.[21]

Interestingly, crystals of **1** which have undergone pyrolytic eliminations maintain their overall shape and size, despite their great loss in weight. A scanning electron micrograph (SEM) of the surface of a particle obtained from thermal decomposition of a single crystal of **1**, heated to 1200 °C under argon, is shown in Figure 5. This needlelike particle has the same hexagonal shape as the original crystal, but the surface appears somewhat coarse and porous. This phenomenon is also observed for crystals of **1** pyrolyzed under air. Note that the latter treatment results in a 75% loss of the crystal's original weight. The BET surface area for the material obtained by pyrolysis of solid **1** in air at 550 °C is 43 m^2 g^{-1}.

Solid-State Thermolysis of $W_2(NHMe_2)_2[O_2Si(O^tBu)_2]_2[OSi(OH)(O^tBu)_2]_2$ (3). Because **3** is extremely air sensitive, the pyrolysis study of this compound was carried out under anaerobic conditions. A TGA analysis of **3** (Figure 6) shows an initial weight

(21) Baxter, D. V.; Chisholm, M. H.; DiStasi, V. F.; Haubrich, S. T. *Chem. Mater.* **1995**, *7*, 84.

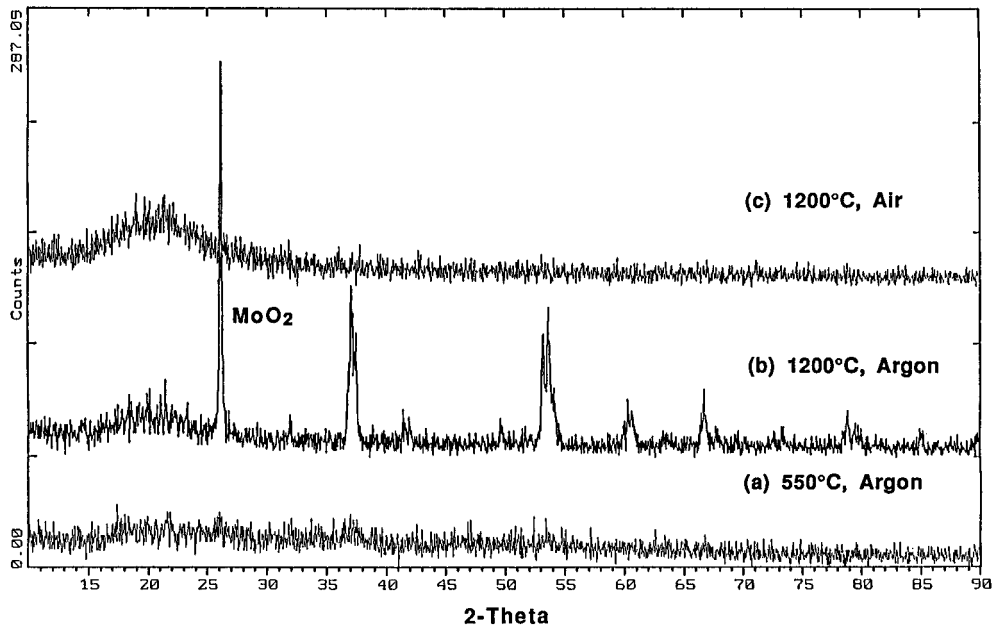

Figure 4. X-ray powder diffraction pattern of the ceramic material derived from **1** by heating to (a) 550 °C, Ar, (b) 1200 °C, Ar, and (c) 1200 °C, air for 1 h.

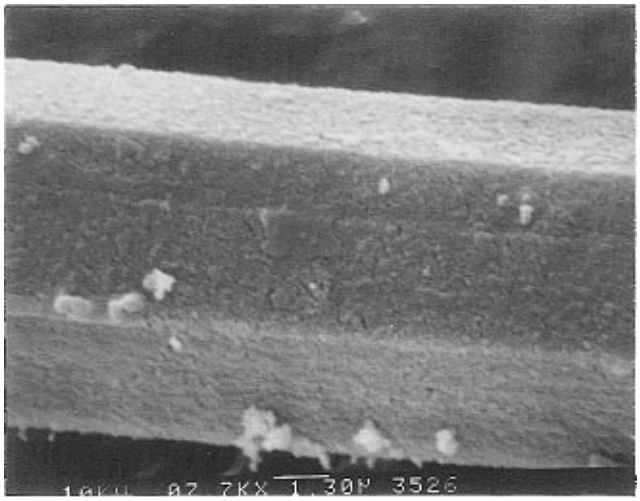

Figure 5. Scanning electron micrograph of a ceramic particle obtained by heating a single crystal of **1** to 1200 °C under argon for 1 h.

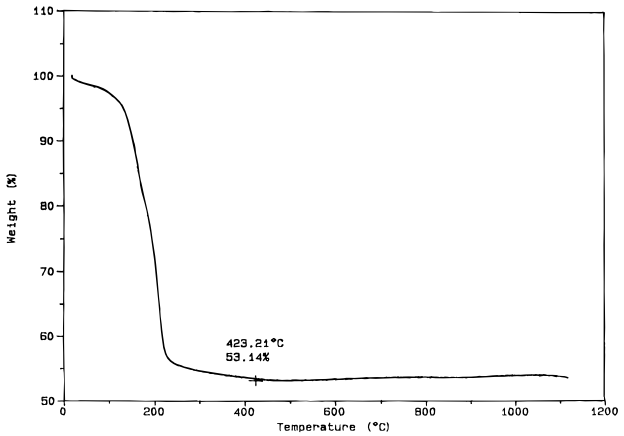

Figure 6. Thermal gravimetric analysis (TGA) trace for $W_2(NHMe_2)_2[O_2Si(O^tBu)_2]_2[OSi(OH)(O^tBu)_2]_2$ (**3**) in argon.

loss starting at only 50 °C, and a decomposition process which becomes quite rapid at 150 °C. The ceramic conversion reaction is complete by 400 °C and results in a 53% ceramic yield. A quantitative NMR analysis of the volatile thermal decomposition products from **3** (at 300 °C under vacuum) revealed the presence of $HNMe_2$, isobutene, and *tert*-butanyl alcohol in a ratio that is consistent with the stoichiometry of eq 5. For comparison the solution phase decomposition of **3** is more complex, giving rise to multiple resonances in the 1.4−1.6 region of the ^1H NMR spectrum.

$$W_2(NHMe_2)_2[O_2Si(O^tBu)_2]_2[OSi(OH)(O^tBu)_2]_2 \xrightarrow[\mathbf{3}]{\Delta} \text{“}W_2Si_4O_{11}\text{”} + 2Me_2NH + {}^tBuOH + 7CH_2{=}CMe_2 + 4H_2O \quad (5)$$

The theoretical yield for a $W_2Si_4O_{11}$ ceramic, 51.05%, is close to that determined from the TGA analysis (53%). Bulk pyrolyses of **3** at 550 and 1200 °C under argon afforded black materials in 56.8% and 49.7% ceramic yields, respectively. The composition of the material obtained by pyrolysis of **1** at 550 °C is consistent with the formula $W_{2.2}Si_4O_{17.4}$, based on elemental analysis (the carbon and hydrogen contents were 1.72 and 0.22%, respectively). An XRD analysis of this material revealed only a very broad peak centered at $2\theta = 20°$ (Figure 7a). When the pyrolysis was carried to 1200 °C, the composition of the resulting material was similar, $W_{2.2}Si_4O_{13}$, except that negligible hydrocarbon was present and it appeared that some deoxygenation had occurred. Consistently, an X-ray analysis of the material heated to 1200 °C (Figure 7b) revealed the presence of crystalline W and WO_2. Peaks with 2θ values of ca. 23.5° and 61.5° could not be assigned with certainty.

Conclusions

In our search for single-source molecular precursors for molybdenum− and tungsten−silica materials, we have synthesized unusual dinuclear molybdenum and tungsten complexes. These compounds possess bridging silanediolato ligands which enforce the most eclipsed geometries yet observed for complexes of these types.

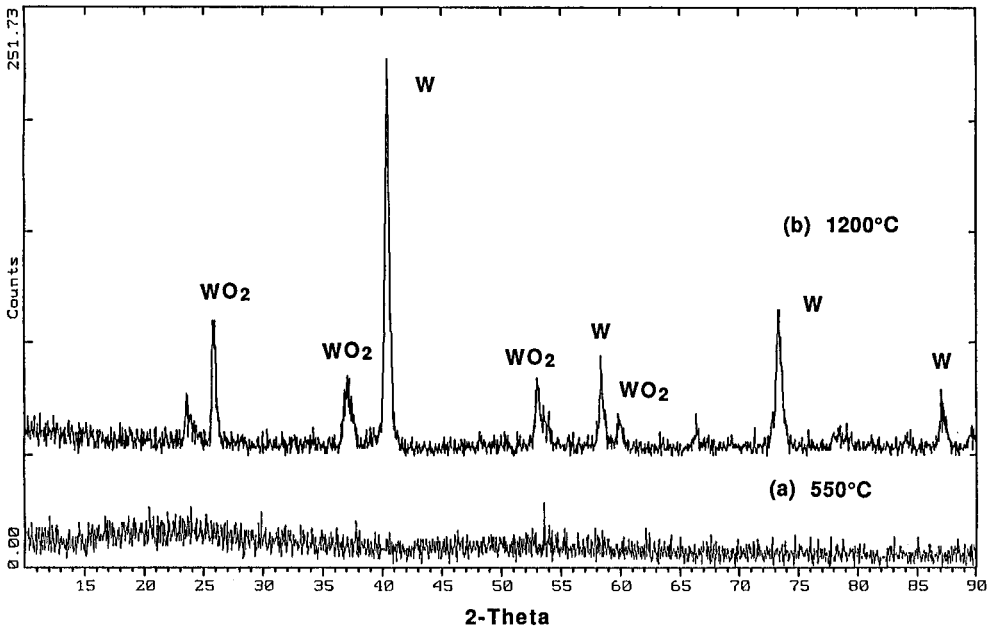

Figure 7. X-ray powder diffraction (XRD) pattern for ceramic material derived from **3** by heating to (a) 550 °C, argon and (b) 1200 °C, argon, for 1 h.

These geometries probably result from steric requirements imposed by the relatively small chelate rings, which cannot distort enough to accommodate more staggered conformations about the M≡M bonds. Complex **1** exhibits pronounced Lewis acidity, such that in the solid state it adopts a chainlike structure via intermolecular dative bonds between the metal and the oxygen atoms of the ligand. This type of interaction may be useful in the design and construction of new organometallic polymers formed via condensation of **1** (or similar complexes) with difunctional donors such as 4,4′-bipyridine or 1,4-benzoquinone. Such possibilities are currently being explored.

Complexes **1** and **2** serve as relatively clean and efficient precursors to metal oxide−silica composite materials. At low temperatures, these complexes pyrolytically transform to oxide materials with elimination of volatile organic species. The molybdenum complex **1** initially gives an amorphous, somewhat porous, "molybdosilicate" which looses MoO_3 at higher temperature. By XRD it appears that at least some of the remaining molybdenum is present as MoO_2, but this element may exist in the material in other forms (e.g., in molybdosilicate structures). Under oxygen, loss of molybdenum at high temperature continues until the molybdenum content reaches very low levels. Interestingly, the pyrolysis of small crystals of **1** occurs with retention of the crystal's shape and size, despite the great loss in weight (75%). This transformation therefore produces needlelike particles of well-defined shape, which are primarily composed of low-density silica.

The tungsten precursor **3** exhibits distinctly different behavior upon thermolysis, with the transformation to ceramic material occurring at much lower temperature. Also, the final tungsten-containing material has a higher transition metal content, with tungsten being present as both WO_2 and W.

The mechanisms of these thermolyses have not been investigated, but it is presumed that the chemistry involved is similar to that observed previously for trialkoxysiloxy complexes of early transition metals.[3a−c,e] Much of the interest in materials of the type described here centers around their use in catalysis.[5] In the next phase of this investigation, we will investigate the activities and selectivities of these materials as oxidation catalysts.

Acknowledgment. This work was supported by the Director, Office of Energy Research, Office of Basic Energy Sciences, Chemical Sciences Division, of the U.S. Department of Energy under Contract No. DE-AC03-76SF00098. We also thank Dr. Fred Hollander of the departmental X-ray facility (CHEXRAY) for determination of the crystal structures, and Claus Lugmair for determination of the surface area.

Supporting Information Available: Tables of crystal, data collection, and refinement parameters, atomic coordinates, bond distances and angles, and anisotropic displacement parameters (22 pages); observed and calculated structure factors (32 pages). This material is contained in many libraries on microfiche, immediately follows this article in the microfilm version of the journal, can be ordered from ACS, and can be downloaded from the Internet; see any current masthead page for ordering information and Internet access instructions.

CM960413S